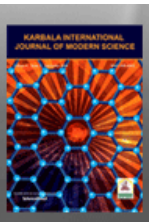

Karbala International Journal of Modern Science

Volume 7 | Issue 2 Article 3

An Implementation of a Multi-Hop Underwater Wireless Sensor Network using Bowtie Antenna

Samuel Ryecroft Mr
Liverpool John Moores University, s.p.ryecroft@2012.ljmu.ac.uk

Andy Shaw Prof
Liverpool John Moores University, A.Shaw@ljmu.ac.uk

Paul Fergus
Liverpool John Moores University, P.Fergus@ljmu.ac.uk

Patryk Kot
Liverpool John Moores University, p.kot@ljmu.ac.uk

Khalid Hashim
Liverpool John Moores University, k.s.hashim@ljmu.ac.uk

See next page for additional authors

Recommended Citation

Ryecroft, Samuel Mr; Shaw, Andy Prof; Fergus, Paul; Kot, Patryk; Hashim, Khalid; Teng, Alex; Moody, Adam; and Conway, Laura (2021) "An Implementation of a Multi-Hop Underwater Wireless Sensor Network using Bowtie Antenna," *Karbala International Journal of Modern Science*: Vol. 7 : Iss. 2 , Article 3.
Available at: https://doi.org/10.33640/2405-609X.2759

An Implementation of a Multi-Hop Underwater Wireless Sensor Network using Bowtie Antenna

Abstract

Water quality is a growing area of research, with more and more focus in the UK and globally on environmental issues and water quality. Current methods of monitoring environmental data such as air quality have continued to develop, spurred on by the growth of the Internet of Things. However, water quality monitoring mainly still depends on manual sample collection. This research presents the first implementation of a multi-hop underwater radio frequency sensor network using bowtie antennas combined with the 433 MHz frequency and a controlled flooding routing approach. The experimental work was conducted in the water reservoir and demonstrates the potential of multi-hop routing in underwater sensor networks to extend range to 19 meters as well as improvements on communication distances from 7 meters previously to 17 meters using radio frequency communications in an underwater environment. Simulated results show that the experimental platform used could enable the long-term deployment of an underwater wireless sensor network that used RF for periods of over a year with support for a 100 sensor node network broadcasting twice daily remaining active for 418 days or a 100 sensor node network broadcasting hourly remaining active for 406 days before any node deaths.

Keywords

Bowtie antenna; sensors; underwater sensor networks; water quality

Authors

Samuel Ryecroft Mr, Andy Shaw Prof, Paul Fergus, Patryk Kot, Khalid Hashim, Alex Teng, Adam Moody, and Laura Conway

1. Introduction

Water quality in the UK, and other parts of the world, is an important issue; suppliers must meet clear requirements for both the water provided at consumer's taps and in water discharged from treatment works [1,2]. UK legislation covers a wide range of water contaminants, such as nitrates, heavy metals, and glyphosates as well as other properties, including odor and color. Sensor technologies have been developed over the years, with sensors developed for a range of contaminants [3]. Sample collection within the water industry still depends on manual methods. A report produced by the drinking water inspectorate identified that in 2018, 0.2% (91 samples of 47,086) failed to meet the standard for odor, 0.18% (87 samples of 47,455) failed to meet the required standard for Iron and 0.68% (78 samples of 11,555) failed to meet the required standards for lead.

Currently, there is no method for the continuous monitoring of water quality in catchment areas for drinking water such as reservoirs or in discharge areas of wastewater treatment works such as rivers and lakes. Monitoring often relies upon manual sample capture, where an individual takes samples from a catchment or discharge site before taking it for testing in a lab, leading to potential delays between a contaminate being introduced and being detected. Additionally, samples are only taken from the edge of a catchment site, meaning there may be delays in the detection of contaminants within the center of the catchment site. There is a need for a novel method of monitoring large catchment sites in more detail and on a more regular basis or even in real-time. A wireless sensor network equipped with sensors capable of detecting the contaminates desired could enable the real-time monitoring of contaminates and potentially alerting to the detection of contaminates when found, allowing the issue to be promptly dealt with.

Over the years, a range of sensors has been developed targeted at common water contaminants, such as a sensor designed by Lin et al. [4], who developed a sensor targeted at the detection of lead and other heavy metals. Other sensors such as that presented by Alahi et al. [5] presented a smart nitrate sensor targeted at the agricultural industry; the work presents an Internet of Things (IoT) connected sensor that is capable of relaying continual nitrate, communicating using radiofrequency in air. Gillett and Marchiori [6] proposed a low-cost continuous turbidity monitor; the sensor used an infrared LED and a TAOS TSL324R light to a frequency converter. With a range of sensor technologies developed, there is a need for a platform that can allow them to be deployed for the monitoring of large bodies of water such as reservoirs.

While many platforms and methods exist for the creation and deployment of wireless sensor networks, however developments in conventional wireless sensor networks have not led to developments in Underwater Wireless Sensor Networks (UWSNs). The lack of a suitable platform for monitoring large water catchment areas such as reservoirs makes monitoring these sites a challenge. Developments in the area of underwater communications using Radio Frequency (RF) [7] have demonstrated communication distances of 7 m in real-world tests at data rates of 1.2 kbps. Previous work by Ryecroft et al. [8] have covered the considerations that need to be undertaken when implementing an underwater sensor network.

Established communication methods in underwater communications include optical and acoustic, with RF, until recently disregarded as not viable. Optical communication offers data rates of up to 500 Mbps and communication distances of up to 150 m with commercial products such as the Bluecomm 5000 series. Optical communications offer many advantages but require alignment to ensure that communication links perform as desired; if nodes become unaligned, it can lead to significant degradation of the link performance. Optical communications only allow for point to point communications, making the implementation of large scale UWSNs a challenge as multiple optical links would be required for each node. Optical communication also depends upon the optical clarity of the water and the turbidity of the water.

Acoustic communications are an alternative and popular communication method in underwater sensor networks, offering long-range communication distances of between 2 km and 6 km with products such as the Teledyne marine 900 series. Acoustic communications offer significantly lower data rates than that of optical and RF, with acoustic communications offering communication speeds of between 80 bps and 15,360bps. Acoustic communications offer some ability to form mesh topology networks, allowing each node to communicate with multiple nodes using a single communication link.

https://doi.org/10.33640/2405-609X.2759

RF communications offer the opportunity of long communication distances without the need for alignment. Other works have used directional antenna designs such as loop antennas forming point to point links similar to optical communications; experimental work by Shaw et al. [9] was able to form communication links at distances of 90 m. Other work has been carried out into using RF to communicate work produced by Lloret et al. [10] achieved communication at distances of 20 cm with communication speeds of up to 11 Mbps using the 2.4 GHz frequency.

Propagation of RF signals in an underwater environment can be impacted by multiple factors; the work of Saini et al. [11] conducted work that showed that higher temperatures lead to a higher attenuation loss within signals meaning that communication distances could be shortened in warmer temperatures, the work also showed that increase in frequency also increases attenuation loss. Work by Smolyaninov et al. [12] examined using a 50 MHz frequency at a range of depths in seawater. The works showed that as depth increased, the communication distance decreased, the work identified that the signal is likely crossing the water–air boundary to propagate rather than passing directly through the water. While this experimental work took place in a saltwater environment: which is more conductive and therefore greater signal attenuation, the findings show that signal will propagate through the air–water boundary, with a similar result likely in less conductive environments such as fresh or brackish water.

Researchers [13,14], have examined the use of bowtie antennas in underwater environments; the work identified an appropriate design for a bowtie antenna that would function in both air and water designed to operate at the 433 MHz frequency. Other works undertaken by Alvertos et al. [15] investigated a bowtie antenna design targeted at the 2.4 GHz frequency. The results from work showed that the designed antenna received a signal strength of −23 dBm at 5 cm of separation; the signal strength then fell in a nearly linear fashion in the order of 0.5 dB/cm. The results showed that bowtie antennas could reach distances of 65 cm underwater using the 2.4 GHz frequency. A bowtie antenna, also known as a Bifin antenna or butterfly antenna, has a bidirectional pattern with broad main beams perpendicular to the plane of the antenna and are linearly polarized, providing a wideband design of the antenna enables the antenna to function at a wider range of frequencies [16], enabling operation in both air and water. Other research has exampled the development of a low-profile bowtie antenna using a 3D printed substrate [17], showing that additive manufacturing techniques can be used to construct low profile antennas. Work has also examined the development of an integrated broadband bowtie antenna on transparent silica substrate; the work showed the fabrication of a bowtie antenna of silica substrate, showing that it can be achieved without unwanted reflection and scattering [18].

The 433 MHz frequency offers several advantages and, therefore, why it was selected for these works; firstly the 433 MHz frequency is an ISM frequency meaning that it is open to use by anyone for Industrial, Scientific, or Medical (ISM) purposes. It is well known that lower frequencies are capable of propagating further in an underwater environment unimpeded, which is why it is important to select a low frequency for these works, with frequencies such as 868 MHz likely to experience higher attenuation than the 433 MHz frequency. There are several ISM frequencies that are lower than the 433 MHz frequency, including 168 MHz, 84 MHz, 40.66 MHz–40.7 MHz, as well as several kHz frequencies. However, the 433 MHz frequency offers several advantages over these other frequencies, the first is the significant increase in the theoretical data rates that can be achieved using the 433 MHz frequency compared to other lower frequencies such as 168 MHz, with 433 MHz offers a higher capacity. Due to the high channel capacity offered by the 433 MHz, many of the shelve transceivers are available, enabling the quick development of prototypes with components that can easily be sourced, giving the 433 MHz frequency an additional advantage.

RF communications in underwater environments offer many advantages, with the possibility of easy setup due to no need for alignment when using RF. Another advantage of RF is that signals can cross the air–water boundary, allowing sensor nodes to be deployed both in water and out of the water. Due to the perviousness of sensor networks that are based around RF, there is also the benefit of mass production transceiver modules that can be used with the appropriate antennas enabling low-cost manufacture of sensor nodes.

The area of wireless sensor networks is widely covered by previous works; one of the most important areas of any sensor network is the routing approach used to relay messages through the network. Protocols such as LEACH and derivatives of it, such as MLEACH [19], are popular protocols and used widely throughout sensor networks. LEACH type protocols use a rotating Cluster Head (CH) to gather data from

nearby nodes before transmitting data to the sink node; in the case of MLEACH, this transmission may use a multi-hop approach to reach the sink node.

LEACH and derivatives such as MLEACH enable the distribution of data transmission within data networks, forming clusters where only one node needs to perform a long-range transmission enabling significant reductions in network power consumption. The results show that using LEACH the first node death occurred over 8 times later than indirect transmission and a static routing protocol, the last node death using LEACH occurs over 3 times later than the last node death in other protocols. MLEACH enables the use of multi-hop routing using LEACH, enabling additional range and allowing for additional network coverage.

MLEACH adds multi-hop routing functionality to the LEACH protocol, allowing cluster heads to transmit to other cluster heads, which can then forward packets on to the sink node when the sink node is not reachable directly.

Another popular routing protocol is PEGISIS (Power-Efficient Gathering in Sensor Information Systems) [20], which uses a chain based approach within the sensor network, each sensor fuses the data received from the previous node with its own data that it has collected, the node then transmits the data onto the next node in the network chain. Results from using PEGISIS shows that the protocol outperforms LEACH by eliminating the overhead of dynamic cluster formations; the results showed that PEGASIS performs better than LEACH by 100%−300% when tested on a range of network sizes and topologies.

Other approaches for sensor network routing include broadcast approaches such as Uncontrolled Flooding and Controlled Flooding [21], in which a network node will transmit a received message to all other reachable nodes. Other approaches include gossiping, which can be used in both broadcast and multicast routing approaches with work such as work produced by Chandra et al. [22] using a gossiping approach to improve the reliability of multicasting. In a multicast routing approach, a single message from one node is distributed to a subset of network nodes within a network, unlike broadcast, where all nodes receive the message.

Network security is an important issue in wireless networks [23,24]. Two core areas within securing network communications: confidentiality and integrity. Confidentiality focuses on ensuring messages cannot be read by unauthorized parties. Integrity ensures that messages can be validated and check to ensure they are from a trusted source.

Confidentiality is a common requirement for wireless sensor networks, enabling information to be communicated without the risk of interception for third parties. Many approaches use symmetric or asymmetric encryption to protect packet payloads, an important consideration in these schemes is the distribution of encryption keys within the network [25,26].

Another important consideration in wireless sensor networks is integrity; in many cases, it is important that a message received can be authenticated to ensure that it was sent from an authentic source; many strategies have been proposed to enable wireless sensor networks to ensure the authenticity of messages. One strategy proposed by Shaheen et al. [27] enabled the confidentiality and authenticity of messages within a wireless sensor network; the approach used symmetric encryption to provide confidentiality, changing the encryption key for each method in a way that is verifiable to provide authenticity. Another approach proposed by Yu et al. [28] proposed an approach of acquiring authentic data within unattended wireless sensor networks, ensuring that messages are transmitted confidentiality and with the ability to ensure integrity.

Underwater wireless sensor networks have a variety of possible applications; the work of Felemban et al. [29] identified several core areas where underwater sensor networks have applications, including monitoring, disaster, and military applications. The works highlighted that there are still issues surrounding low data rates of RF communications and the need to be able to have reliable and robust network design strategies that allow for easy deployment in underwater environments.

2. Materials and methods

The experimental work carried out used bowtie antennas based on the antenna design presented in previous work presented by Abdou et al. [13] which used similar dimensions; the antenna was produced using a chemical etching process [7]. Each antenna had a top lamination layer of epoxy resin to ensure that the poles of the antenna were insulated and unable to short when submerged; the lamination also protected the antenna surface from abrasion and damage. Fig. 1 shows the design and measurements of the antenna. Fig. 2 shows the antenna radiation pattern radiating at 433 MHz.

The experimental works used a HopeRF RFM69hw transceiver module using the 433 MHz frequency. The

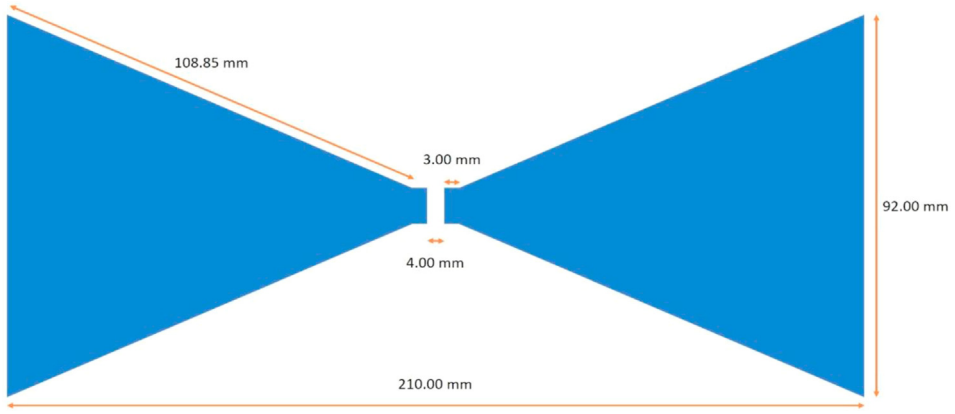

Fig. 1. Bowtie antenna design and measurements.

HopeRF HW69 module provides a transmission power of +20 dBm and a receiving sensitivity of up to −120 dBm. The RFM69hw module offers a range of features, including a range of modulation techniques such as OOK, FSK GFSK, MSK, and GMSK. The module offers baud rates of up to 299 kb/s. The experimental works opted for using OOK with a baud rate of 1.2 kb/s, this combination selection was made based on previous field trials showing that the 1.2 kb/s baud rate with OOK modulation offers better communication distances in the work examined, although in future works, it may be possible to use a dynamic data rate depending upon separation distances.

A baud rate of 1.2 kb/s enables a longer transmission rate than higher baud rates would, as shown with the Shannon-Hartley Theorem [30,31]. The theorem shows the relationship between the signal to noise ratio and the maximum baud rate that can be used to communicate, the signal to noise ratio is impacted by the separation distance between sensor nodes, with larger distances reducing the strength of the signal. Based upon Shannon-Hartley, using a lower baud rate will enable a larger communication distance to be achieved.

The experimental work used the RFM69hw as the transceiver module based on several factors, including the compatibility of the module with the Arduino

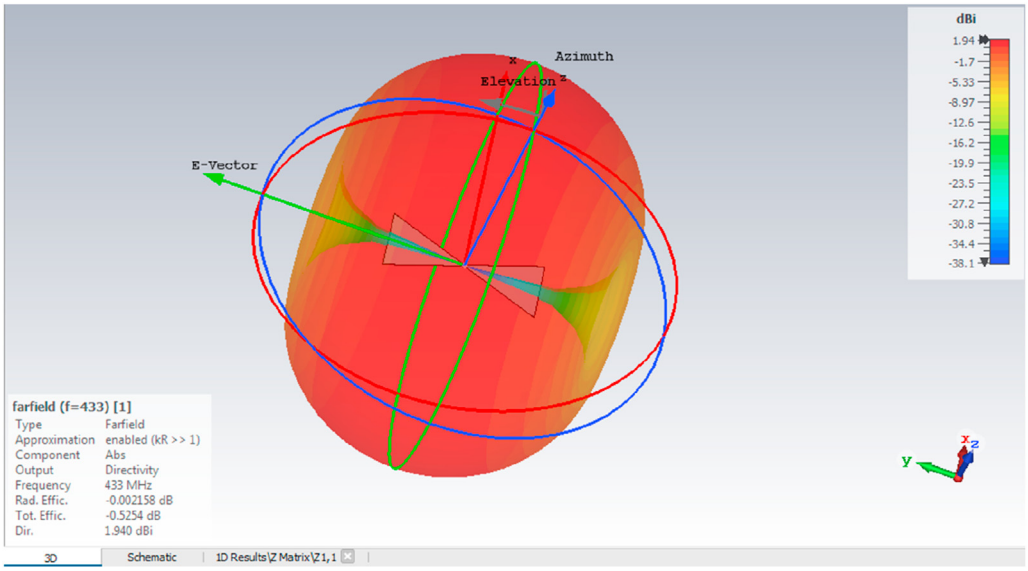

Fig. 2. Bowtie antenna radiation pattern at 433 MHz.

platform, including multiple software libraries, to enable the development of the required firmware. The module was also selected due to its low-level sensitivity to levels of up to −120 dBm and high transmission power of up to +20 dBm. These factors combined with the additional features offered by the module, including hardware-accelerated AES encryption, built-in packet mode with features including sync word detection and node addressing.

As discussed, security is an important aspect of wireless sensor networks; while security can take many forms, one form is confidentiality to ensure that messages cannot be intercepted by a middleman attacker and read. To demonstrate how confidentiality can be ensured, the developed firmware makes use of the hardware AES encryption module to ensure that all communications are encrypted. The method uses a simple static shared decryption key, although later iterations could examine the use of more complex key management approaches.

The packet structure used is based around the base packet used by the RFM69hw although parts of this packet are abstracted from the software and are handled at a hardware level. Fig. 3 shows the packet structure including abstracted hardware bytes that are used during experimentation.

The transceiver module was connected to an Atmel 328p microcontroller using an SPI bus. Each sensor node used a TSYS01 temperature sensor and an MS5837-30BA depth sensor, connected to the microcontroller using the I^2C communication protocol. The temperature and depth sensors were used to acquire data that was then communicated through the network, providing an example of real-time sensor data being collected. Fig. 4 shows a block diagram of the circuit developed and used for the experimental works. Fig. 4 shows a photo of the circuit board used without the antenna attached.

Fig. 5 shows the flow of the firmware used on the microcontroller during experimental works. The firmware developed the setup of the microcontroller to communicate with the sensors and transceiver module before entering a continuous loop where incoming messages were checked for and readings transmitted as required.

The firmware used on the sensor platform for experimental works was implemented using the C++ programming language using the Arduino software libraries and boot loader. The sensor firmware uses a time delay to schedule when readings are transmitted; once a reading is due to be sent, the firmware interacts with each of the attached sensors to the node using the I2C protocol and the supporting communication libraries. Once the readings are taken, the firmware generates a new message ID before uploading the message IDs used by the sensor node. Once complete, the sensor node transmits the data packet to the wider network, where the controlled flooding protocol manages the flow of the packet through the network.

The routing protocol was an implementation of controlled flooding, with each message being given a unique message ID, the message ID used was a counter prefixed with the unique ID of the node, once the counter reaches 99, it rolls over to 0 again, when a message is transmitted the unique ID is included to distinguish the message from others transmitted within the network. Alternatively, a multicast routing protocol could have been applied; however, there is more complexity in implementing it, which could lead to issues during initial field trials; there is also a chance that in a multicast routing protocol implementation, there is not a viable path to a target sink node whereas with controlled flooding the message will always be received by the sink node if there is a viable path from the transmitter to the receiver.

The implemented approach allows all sensor nodes to receive messages transmitted within the network, meaning that the only limitation upon a node receiving messages is physical due to the decay of the transmission signal. Upon receiving a message, a sensor node decides to either retransmit a message or not. It is this part of the algorithm that distinguishes Flooding

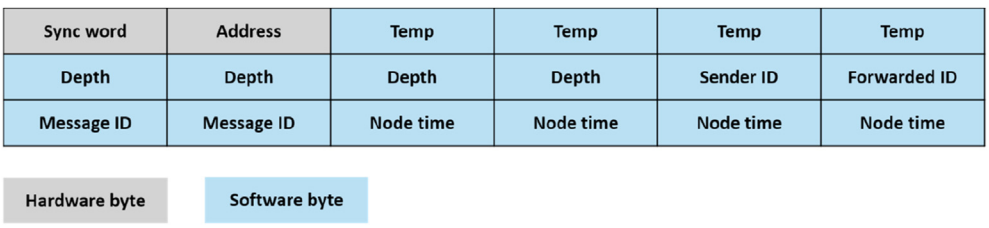

Fig. 3. Packet structure used during experimentation, including packets managed at a hardware level.

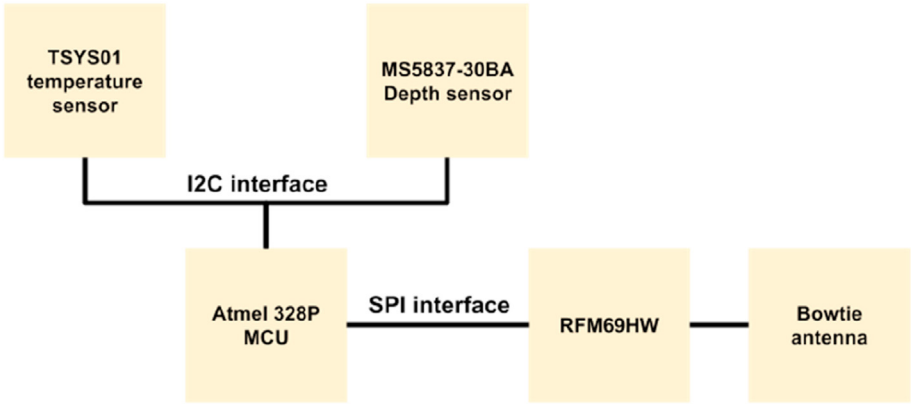

Fig. 4. A block diagram of the circuit used during experimental works.

routing from Controlled Flooding, with flooding retransmitting all messages. The sensor node decides if a message should be retransmitted based upon the message ID, the sensor node keeps the state of the last message ID it retransmitted for each known sensor node, by deriving the sensor node ID from the message ID, in cases where the message has been transmitted previously, the sensor node will not retransmit the

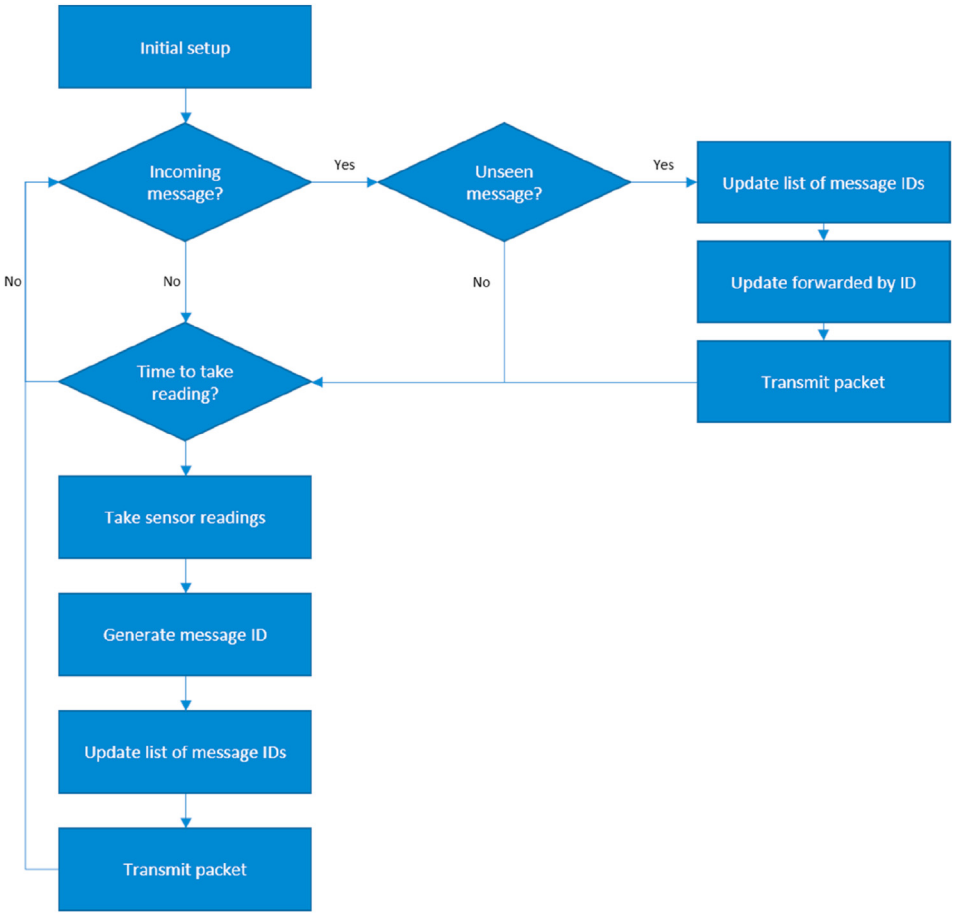

Fig. 5. Flow chart of microcontroller software.

Fig. 6. (a) An example of the sensor node used during experimental works (b) An image of the experimental site where fieldwork was undertaken.

message again; in cases where the sensor node has not to retransmit the message already then, the sensor node will transmit the message.

Each sensor node used an underwater enclosure constructed from acrylic tubing with aluminum end-caps manufactured by Blue Robotics and supplied by the Robot shop, Hethersett, United Kingdom. The PCBs were mounted in the enclosures and connected to a 12 V lead-acid battery. The housing was connected to a polyfoam buoy and a mushroom anchor. The buoy was connected to the housing using nylon rope 50 cm in length, allowing the housing to be submerged to a depth of 50 cm, making the buoy completely separate and isolated from the sensor node. The buoyancy of the buoy was enough to support the weight of the attached anchor, which was used to counter the buoyancy of the housing; the buoy served only to show the location of the submerged sensor nodes for the purposes of the experiment undertaken an example of the sensor node can be seen in Fig. 6a.

Experimental work took place at Hurlstone reservoir, a water catchment site for United Utilities; Fig. 6b shows the layout of how sensors were located during the experimental work. S1 was anchored in the water close to the edge and connected to an FTDI adapter intern connected to raspberry pi for data capture. S1 was placed further out in the reservoir and was moved to increase and decrease the distance of separation between S2, S2, and S3. A third sensor (S3) was placed outside of the water at the edge simulating an example of a sensor node that was no longer submerged due to the changing depth of the reservoir and remained in the same location throughout the experiments.

Table 1
A table of results from field testing for a range of distances.

Distance	Received signal strength (dBm)	Received signal strength Standard deviation	Node 1 forwarded
4	−90.17	0.69	False
5	−92.83	0.68	False
6	−100.34	0.47	False
7	−99.00	0.58	False
8	−105.67	1.57	False
9	−109.17	0.37	False
10	−101.17	0.90	False
11	−103.50	1.50	False
12	−106.67	1.25	False
13	−103.67	0.47	False
14	−107.34	1.70	False
15	−107.67	0.75	False
16	−106.17	0.37	False
17	−108.17	0.69	False
18	NA	NA	True
19	NA	NA	True

3. Experimental results and discussion

Table 1 shows the mean signal strength for each of the distances tested during the fieldwork as well as the standard deviation of each of the distances tested with 7 readings taken per distance. The results in the table show that the first sensor node was able to communicate directly with the sink node up to 17 m. The results show that after the point of 17 m, the data was relayed through the second node that was placed out of water.

The results show a significant improvement over previous results where 7 m of separation between nodes was achieved. These improvements in separation distance could be due to several possibilities. The first possibility is that the previous testing site was situated near metallic objects; these objects could have increased the signal lost during transmission. Another possibility is that the shallow nature of the previous testing site could have caused a higher signal to noise ratio due to reflected signals. The Shannon Hartley theorem shows that the signal to noise ratio can impact the maximum feasible data rate of the channel; the deeper testing environment of the testing site could have reduced the impact of reflected signals. Alternatively, due to the built-up nature of the testing area, is it possible that there was increased RF interference from other nearby devices.

Fig. 7 shows a plot of the signal strength against the distance; as expected in general, a reduction of signal strength as the distance increases can be seen. This is in line with what would be expected as it is well understood that as distance increases, the signal strength will decrease; the plot highlights a few distances where readings do not follow the general pattern; however, a pattern is clearly discernible in the plot.

The use of multi-hop routing provides an opportunity to increase the range of sensor networks deployed in underwater sensor networks. Rather than the sink node needing to be within 17 m of all network nodes, the usage of multi-hop routing allows this distance to be extended, with the use of a single hop which enables the sink node to be 34 M away from the sink node in a best-case scenario. With careful planning of node placements, it is possible to cover larger areas with a UWSN using a multi-hop routing protocol with RF communications. In this study, a controlled flooding approach to transmit messages to all nodes through the network was used; this works well where nodes are sparse, a network topology is not clear, and there is the possibility of changes in the route messages take due to movement or the loss of nodes within the network. In cases where there is a larger density of nodes, other approaches such as LEACH, MLEACH or PEGISIS could provide a better routing approach to optimize power consumption in the network to improve the overall network lifetime.

The software developed for the experimental work did not consider power consumption due to the software being targeted for experimental work only. It is possible to make significant improvements to the

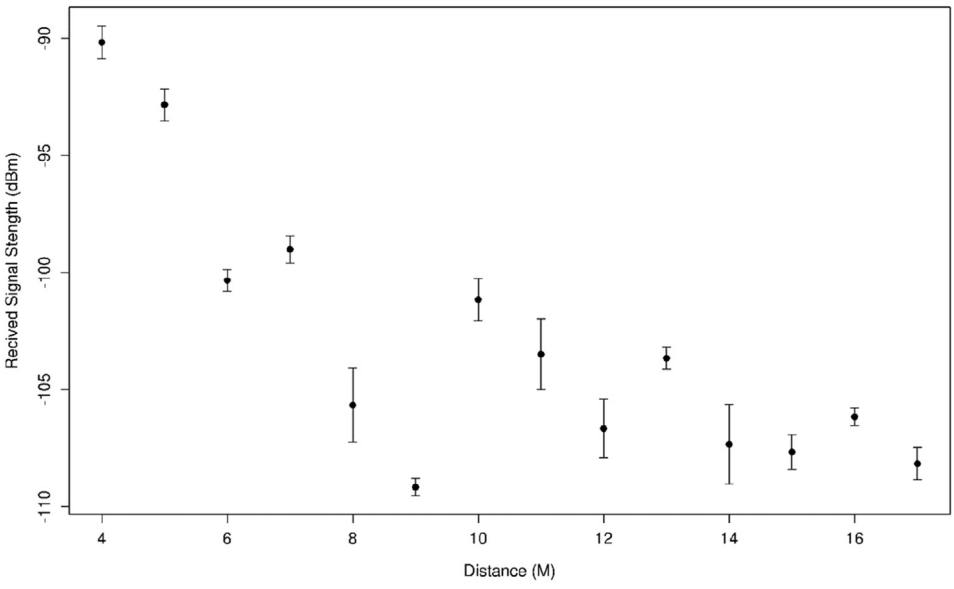

Fig. 7. A plot of signal strength against distance.

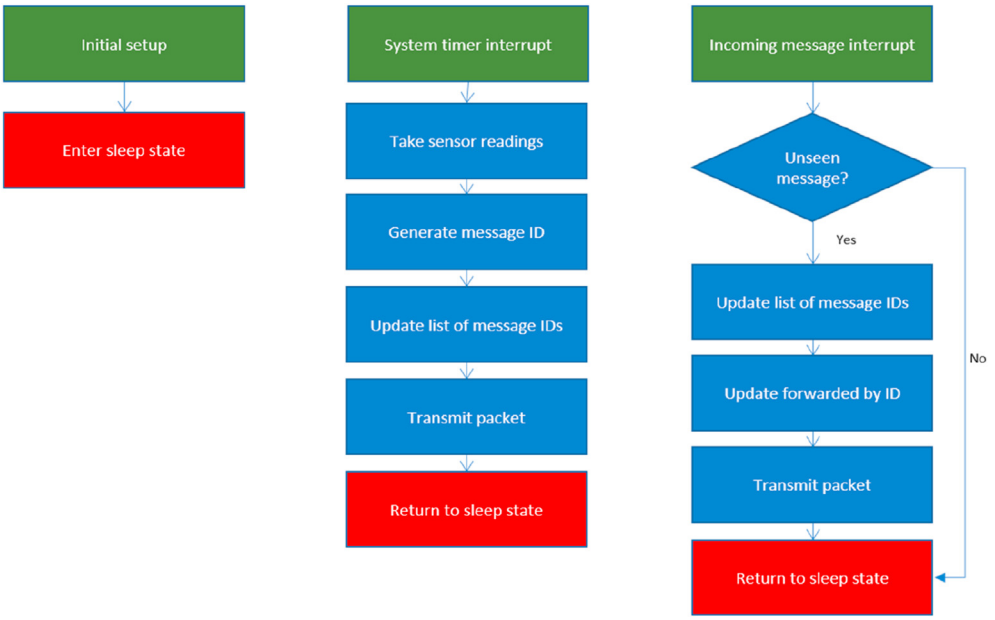

Fig. 8. Example flowchart for interrupt-driven approach.

power consumption of the software by using features such as hardware sleeps and using interrupts rather than polling the transceiver module for messages. It would also be possible to use a system timer to generate an interrupt to take and transmit a sensor reading allowing for further uses of a sleep state.

Fig. 8 shows an improved flow chart of the software that could be used to significantly improve the energy consumption of the platform developed, therefore increasing the lifetime of the network.

Using an interrupt-driven approach, a significant amount of power can be saved by making use of a low power sleep state of not only the microcontroller, but also other low power states that may be available such as the low power state that the RFM69HW module supports, allowing the module to still receive data, but enabling reduction in power consumption. The use of interrupts also enables the removal of the long-polling that is otherwise required to ensure that new radio transmissions are received and processed and that data is transmitted at the correct intervals.

Based on the previous works of Smolyaninov et al. [12] it can be inferred that communications are primarily dominated by surface electromagnetic waves. Based on these previous works, it can be assumed that as the depth of the sensor nodes increases, the communication distance that is achievable will decrease due to the signal propagating through more water before reaching the surface. An examination of how this impact achievable communication distances. Previous work has shown that the attenuation of the signal is significantly impacted by the conductivity of water, meaning that this combined with the depth at which the signal is transmitted.

Other works have shown that the impact of factors such as depth, temperature, and conductivity all have an impact on how far signals are able to propagate through the water [11,12]. The experiments conducted showed how a network node submerged 50 cm into a reservoir of deep water can travel, the works were undertaken in raw water with a temperature of 17.5 °C. Based on the literature, it is clear that factors such as salinity and temperature of the water that communications are made in as well as the depth at which communications are made, will all impact the distances achievable.

Table 2
Current consumption measurements for the developed platform.

State	Current consumption at 12 V (mA)
Sleep	1.99
Transmit	26.97
Receive	8.47

4. Simulation of an underwater wireless sensor network

Based on the experimental fieldwork undertaken above, simulations were created to examine how well

underwater wireless sensor networks would operate within site such as Hurlstone reservoir; the site fieldwork was undertaken at.

The simulation used power consumption figures captured directly from the developed platform used throughout the experimental work. The power consumption figures were captured for three states; low power sleep, transmit and receive using a Keithley DMM7510 benchtop multimeter. The measured current consumption is shown in Table 2.

For simulation purposes, several use cases were examined, with use cases of transmissions for hourly, twice daily, and daily transmissions. Energy consumption was calculated in Joules using the formula shown in equation (1); all calculations assumed a supply voltage of 12 V as current consumption was measured at 12 V.

$$E = T \times I \times V \quad (1)$$

E = energy (J)
T = time (S)
I = Current (A)
V = Voltage (V)

Table 3 shows the total energy consumption of the platform during a sleep state that lasts from 1 min to 1 week in joules. Data was collected for broadcasting a range of packet sizes to assess how packet size affects energy consumption for transmission and reception. While the current consumption remains the same for packet size, the duration will differ due to the amount of time required to transmit and receive the packet, which will impact the total energy consumption. The duration for transmitting and receiving data was found to be identical to 3 significant figures; for simplicity, the same value has been used for both transmitting and receiving data, the duration and associated energy costs can be seen in Table 4.

A simulation application was developed in the Java programming language that randomly generated a wireless sensor network with the same broadcast routing approach used in the field; the simulation application took the number of nodes, dimensions, and maximum transmission range of nodes as parameters. The simulation used the consumption figures presented in Tables 3 and 4 to provide simulated results based on a working platform.

Table 3
Duration and energy usage in joules for sleep states.

Use case	Duration (s)	Energy usage (j)
One transmission per minuet	60	1.43
One transmission per hour	3600	85.97
One transmission per 12 h	43,200	1031.62
One transmission per 24 h	86,400	2063.23
One transmission per 168 h	604,800	14442.62

Table 4
Duration and energy usage in joules for transmission and receiving data.

Packet size (Bytes)	Duration	Transmit energy usage (j)	Receive energy usage (j)
8	0.045	0.015	0.005
16	0.167	0.054	0.017
32	0.252	0.082	0.026
64	0.463	0.150	0.047
128	0.988	0.320	0.100

The simulation approach used the same broadcast routing method that we applied during the fieldwork; while other protocols such as multicast, LEACH and PEGISIS would provide an improvement to power consumption figures, the simulation would then not reflect the platform presented in section 3.

The simulations for each communication interval and node number were run 2000 times, each time on a new randomly generated network layout where nodes were randomly placed within the boundaries of the simulation. A sensor node within the simulation was placed no closer than 1 m to another sensor node to represent a more realistic deployment where nodes are unlikely to be placed extremely close together, 1 m was also used as this ensured that there was enough space within the boundaries of the simulation for a random sensor network to be generated with larger numbers of nodes.

The simulation work used parameters based upon the data collected during fieldwork described within section 3. The simulation used a communication distance of 15 m, based upon a communication distance achieved of 17 m in fieldwork, with the distance

Table 5
Static simulation parameters.

Parameter	Value
Simulation space width (m)	260
Simulation space height (m)	360
Simulations run	2000
Node communication range (m)	15
Battery voltage (V)	12
Battery amp hour rating (Ah)	20
Battery charge (J)	864,000
Packet size (Bytes)	64

shortened slightly to represent the likely reduction in communication distances that may be observed due to an increase in signal to noise ratio. The simulation also used the approximate size of the Hurlstone revivor, where fieldwork was undertaken to represent the boundaries of the simulation space.

The simulation made use of power consumption figures used in the simulation were based upon the power consumption figures measured for one of the sensor nodes in a sleep state, transmitting state and receiving state when supplied with 12V with the values found shown in Table 2. The simulation also used the measured duration of the transmitting and receiving state for a variety of packet sizes to ensure an accurate representation could be made within the simulation; for simplicity, the simulation results presented to use a packet size of 64 bytes, a similar size to that used during experimental works.

All simulations used the following static configuration parameters presented in Table 5; the dimensions used during simulations are based on the approximate size of the Hurlstone reservoir. The simulations run represents the number of simulations run for each defined parameter set.

The Simulations run parameter represents the number of simulations that were undertaken for each combination of the number of nodes deployed and transmission interval.

The node communication range represents the maximum distance that simulated sensor nodes can communicate. The value used was based on a slightly reduced distance that was achieved in the presented experimental field works above. The distance was reduced by 2 m to account for a slight increase in the signal to noise ratio that would likely be experienced in a larger deployment of an underwater sensor network.

The battery voltage and amp-hour ratings were taken based on available products, with a 12 V being used due to the current consumption figures being taken while a 12 V 20 Ah rating was used based on lead-acid batteries that are readily available. This simulation assumes that the battery will always remain at 12 V rather than fluctuating due to the current draw and charge.

Simulations were run for five different quantities of nodes being deployed; 100, 200, 300, 400, and 500. Simulations examined three different intervals of hourly, twice-daily, and daily, which could have applications in industry for routing monitoring as well as monitoring of contamination incidents. In total, 15 simulation cases were examined, with every permutation of node quantities and transmission intervals being examined.

Table 6 presents the simulation results for all simulation cases run with the number of days before the first node; 25%, 50%, 75%, and 100% of nodes run out of power.

The results show that in call cases, the total network lifetime of the network is always either 418 days or 419 days; this is due to the fact that once a particular number of sensor network nodes have died within the network, there is a significant reduction in the number of transmissions each node has to transmit as there are fewer if any messages for the sensor node to transmit. The simulation shows that there is a point at which there is likely one a few sensor nodes left, all of which

Table 6
Simulation results.

Nodes	Transmission interval	First node death (days)	25% nodes dead (days)	50% nodes dead (days)	75% nodes dead (days)	100% nodes dead (days)
100	Hourly	406	415	417	418	418
200	Hourly	371	406	413	416	418
300	Hourly	278	376	398	411	418
400	Hourly	148	274	331	389	418
500	Hourly	89	160	207	265	418
100	Twice daily	418	418	419	419	419
200	Twice daily	414	418	419	419	419
300	Twice daily	400	415	417	418	419
400	Twice daily	363	397	409	416	419
500	Twice daily	320	359	372	388	419
100	Daily	419	419	419	419	419
200	Daily	417	419	419	419	419
300	Daily	410	417	418	419	419
400	Daily	391	406	411	417	419
500	Daily	363	386	393	402	419

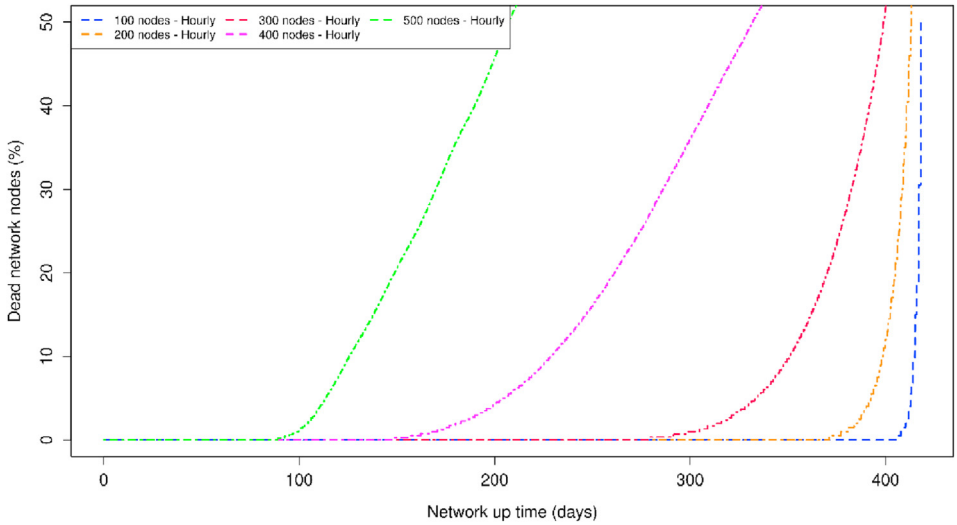

Fig. 9. A plot of the hourly results from the simulation results.

are unable to communicate and therefore will die at the same rate regardless of the number of nodes the network started with or the number of transmissions each node sends. This result indicates that the main power consumption within the network is related to the forwarding of messages due to the broadcast routing approach applied.

The results indicated that used cases such as every 12 h or every day provided a significant lifetime duration of over 300 days in both cases with 500 sensor nodes. These types of data capture offer significant improvements in the frequency of sampling that is currently taken using manual methods within the water industry, enabling more regular readings to be taken without the need for manual sample collection while providing a significant network lifetime.

Figs. 9–11 shows a plot of simulation results using the base parameters presented in Table 5, simulations were run for 100, 200, 300, 400, and 500 sensor nodes for the following scenarios, once per day transmission, twice-daily transmission, Hourly transmissions. As expected, a reduced number of transmissions provides longer overall network lifetimes. The simulations results show that in all cases, as the number of network

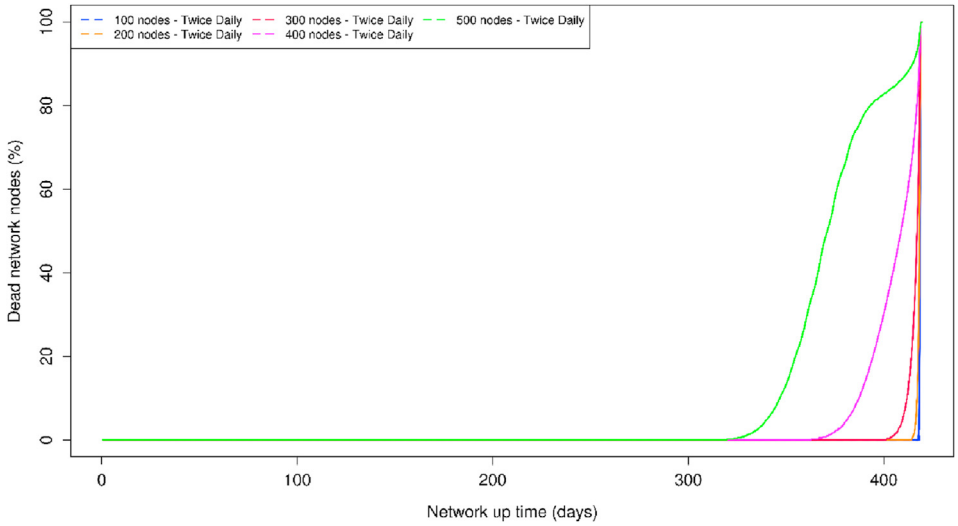

Fig. 10. A plot of simulation results of twice-daily transmission.

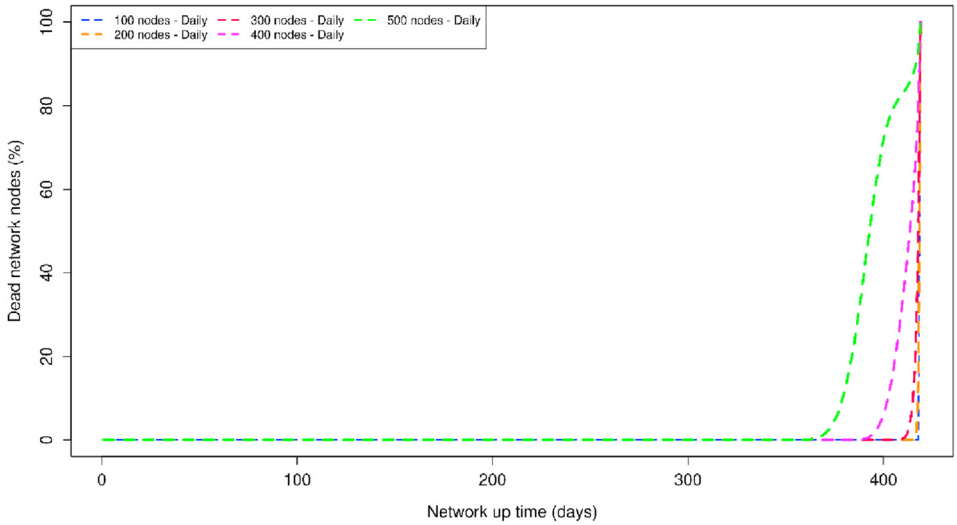

Fig. 11. A plot of simulation results for daily transmission.

nodes increases, the point at which sensor nodes begin to die off starts sooner; this is due to the broadcast topology used in the simulation, as the more sensor nodes within the network then more times a sensor node is likely to broadcast additional messages received from other sensor nodes.

The results for data capture on an hourly basis show significant possibility, enabling high-resolution data capture for shorter durations. This duration of network lifetimes could be of use to the water industry for managing ongoing events or for surveying water catchment areas for contaminates in fine detail, identifying where contaminates originate from and how they spread through a reservoir.

The results indicate that, as expected, the sleep power consumption of the developed platform plays a significant role in the overall network lifetime; this is especially clear when the reading intervals are higher such as the 12 h and 24-h sampling periods. Improvements made to the platform to enable a more energy-efficient sleep state could lead the way for even longer durations; the use of energy harvesting technologies could also allow for significantly longer deployment durations, allowing power to be harvested in part or fully from the environment.

The results show that for more regular readings, the broadcast routing approach and transmission energy consumption start to reduce network lifetime significantly. It is possible that future approaches could improve this significantly, either through a more efficient routing protocol such as LEACH or PEGISIS as well as managing transmission power used more efficiently through the transceiver to reduce power consumption during transmission depending on the distance the node needs to transmit.

The simulations presented based on the platform are a significant scaling of the work presented in section 3, with power consumption figures and communication distances taken from an existing real-world platform. The simulations have been based upon these figures and show the potential network lifetime that could be achieved with the platform presented in section 3.

5. Conclusions

The fieldwork shows that a multi-hop routing approach applied in an underwater sensor network in a scenario does work and can be used to extend the range of a network. The fieldwork also presents the usage of sensor nodes deployed both in and out of the water and how they can work together to take advantage of RFs ability to cross the air–water boundary to increase the communication distance of the wireless sensor network.

The work presents simulation results based on undertaken fieldwork and a real-world communication platform capable of underwater wireless communication using the 433 MHz frequency to project network lifetimes of up to 391 days before the first node death using a daily transmission of data with 400 sensor nodes or up to 148 days before the first node death transmitting data every minute using 400 sensor nodes, with results based upon a tried and tested platform.

The work presented shows the novel deployment of real-world deployment of an underwater wireless sensor network using radio frequency communications and multi-hop routing to communicate data at a distance between sensor nodes with supporting simulations results to project potential network lifetimes. The work presented shows that a multi-hop communication in a small underwater wireless sensor network, with a platform that simulations show, could be used to deploy a largescale sensor network for a prolonged period of time. Further work in the future could investigate the possibility of larger-scale deployments over a prolonged period of time to further prove the viability of a large scale underwater wireless sensor network as well as the possibility of introducing a variable data rate to maximize the communication speeds achievable.

This paper presents the first implementation of an underwater wireless broadcast sensor network using a controlled flooding routing approach with real-world fieldwork undertaken in a large deployment environment. The results presented show a significant improvement in communication distances achieved with distances of up to 17 m of direct communication between sensor nodes at bit rates of 1.2 kbps, which can be extended through the use of an intermediary sensor node which was shown to increase the range in these experimental works to 19 m although further distances may be achievable. This is a significant improvement over previous work conducted in the Liverpool Canal, where a distance of 7 m for direct communication was achieved [7].

Author contributions

Conceptualization, AS and PK; Formal analysis, SR, PF and KH; Funding acquisition, A.M. and LC; Investigation, SR, PF and KH; Methodology, AS and PK; Software, SR; Supervision, AS, PF and PK; Validation, SR, PF, KH and AT; Writing − original draft, SR and PK; Writing − review & editing, AS, KH, A.M., LC and AT.

Funding

This research was funded by United Utilities, Warrington.

Conflict of interest

The authors declare no conflict of interest.

References

[1] B. Abdulhadi, P. Kot, K. Hashim, A. Shaw, M. Muradov, R. Al-Khaddar, Continuous-flow electrocoagulation (EC) process for iron removal from water: experimental, statistical and economic study, Sci. Total Environ. 756 (2021) 1−16.

[2] K.S. Hashim, A. Shaw, R. AlKhaddar, P. Kot, A. Al-Shamma'a, Water purification from metal ions in the presence of organic matter using electromagnetic radiation-assisted treatment, J. Clean. Prod. 280 (2021) 1−17.

[3] S.P. Ryecroft, A. shaw, P. Fergus, P. Kot, K. Hashim, L. Conway, A novel gesomin detection method based on microwave spectroscopy, in: Proceedings of 12th International Conference on Developments in eSystems Engineering (DeSE), Kazan, Russia, Year, 2019.

[4] W.-C. Lin, Z. Li, M.A. Burns, A drinking water sensor for lead and other heavy metals, Anal. Chem. 89 (2017) 8748−8756.

[5] M.E.E. Alahi, L. Xie, S. Mukhopadhyay, L. Burkitt, A temperature compensated smart nitrate-sensor for agricultural industry, IEEE Trans. Ind. Electron. 64 (2017) 7333−7341.

[6] D. Gillett, A. Marchiori, A low-cost continuous turbidity monitor, Sensors 19 (2019) 3039.

[7] S. Ryecroft, A. Shaw, P. Fergus, P. Kot, K. Hashim, A. Moody, L. Conway, A first implementation of underwater communications in raw water using the 433 MHz frequency combined with a bowtie antenna, Sensors 19 (2019) 1813−1823.

[8] S.P. Ryecroft, A. Shaw, P. Fergus, P. Kot, M. Muradov, A. Moody, L. Conroy, Requirements of an underwater sensor-networking platform for environmental monitoring, in: The 11th International Conference on Developments in eSystems Engineering (DeSE), Cambridge, UK, 2018, pp. 95−99.

[9] A. Shaw, A.I. Al-Shamma'a, S.R. Wylie, D. Toal, Experimental investigations of electromagnetic wave propagation in seawater, in: The European Microwave Conference, Manchester, UK, 2006, pp. 572−575.

[10] J. Lloret, S. Sendra, M. Ardid, J.J.P.C. Rodrigues, Underwater wireless sensor communications in the 2.4 GHz ISM frequency band, Sensors 12 (2012) 4237−4264.

[11] P. Saini, R.P. Singh, A. Sinha, Path loss analysis of RF waves for underwater wireless sensor networks, in: Proceedings of 2017 International Conference on Computing and Communication Technologies for Smart Nation (IC3TSN), 2017, pp. 104−108.

[12] I.I. Smolyaninov, Q. Balzano, C.C. Davis, D. Young, Surface wave based underwater radio communication, IEEE Antenn. Wireless Propag. Lett. 17 (2018) 2503−2507.

[13] A. Abdou, A. Shaw, A. Mason, A. Al-Shamma, J.D. Cullen, S. Wylie, M. Diallo, A matched Bow-tie antenna at 433MHz for use in underwater wireless sensor networks, J. Phys. Conf. 450 (2013) 2048.

[14] A.A. Abdou, A. Shaw, A. Mason, A. Al-Shamma, S. Wylie, J.D. Cullen, Wireless sensor network for underwater communication, in: IET Conference on Wireless Sensor Systems (WSS), London, UK, 2012, p. 11.

[15] N. Alvertos, E. Karagianni, D. Vardakis, T. Mpountas, D. Kaklamani, Bow-tie antenna for underwater wireless sensor networks, in: International Workshop on Antenna Technology: Small Antennas, Innovative Structures, and Applications (iWAT), Athens, Greece, 2017, pp. 323−326.

[16] W.L. Stutzman, G.A. Thiele, Antenna Theory and Design, John Wiley & Sons, Hoboken, 2012.

[17] M. Mirzaee, S. Noghanian, I. Chang, Low-profile bowtie antenna with 3D printed substrate, Microw. Opt. Technol. Lett. 59 (2017) 706−710.

[18] X. Zhang, C. Chung, S. Wang, H. Subbaraman, Z. Pan, Q. Zhan, R.T. Chen, Integrated broadband bowtie antenna on transparent silica substrate, IEEE Antenn. Wireless Propag. Lett. 15 (2016) 1377−1381.

[19] R.K. Kodali, A. VSK, S. Bhandari, L. Boppana, Energy efficient m- level LEACH protocol, in: International Conference on Advances in Computing, Communications and Informatics (ICACCI), Kochi, India, 2015, pp. 973−979.

[20] S. Lindsey, C.S. Raghavendra, PEGASIS: power-efficient gathering in sensor information systems, in: IEEE Aerospace Conference, MT, USA, 2002, pp. 1125−1130.

[21] J.F. Kurose, K.W. Ross, Computer Networking a Top-Down Approach, Pearson, New York, 2013.

[22] R. Chandra, V. Ramasubramanian, K. Birman, Anonymous Gossip: improving multicast reliability in mobile ad-hoc networks, in: The 21st International Conference on Distributed Computing Systems, Mesa, AZ, USA, 2001, pp. 273−275.

[23] A.S.K. Pathan, L. Hyung-Woo, H. Choong Seon, Security in wireless sensor networks: issues and challenges, in: The 8th International Conference Advanced Communication Technology, Phoenix Park, Korea (South), 2006, pp. 1043−1048.

[24] A. Karakaya, S. Akleylek, A survey on security threats and authentication approaches in wireless sensor networks, in: The 6th International Symposium on Digital Forensic and Security (ISDFS), Antalya, Turkey, 2018, pp. 1−4.

[25] F. Gandino, R. Ferrero, M. Rebaudengo, A key distribution scheme for mobile wireless sensor networks: q-s-Composite, IEEE Trans. Inf. Forensics Secur. 12 (2017) 34−47.

[26] R.M. Alshammari, M.K. Elleithy, Efficient and secure key distribution protocol for wireless sensor networks, Sensors 18 (2018) 1−25.

[27] J. Shaheen, D. Ostry, V. Sivaraman, S. Jha, Confidential and secure broadcast in wireless sensor networks, in: IEEE 18th International Symposium on Personal, Indoor and Mobile Radio Communications, Athens, Greece, 2007, pp. 1−5.

[28] C.-M. Yu, C.-Y. Chen, C.-S. Lu, S.-Y. Kuo, H.-C. Chao, Acquiring authentic data in unattended wireless sensor networks, Sensors 10 (2010) 2770−2792.

[29] E. Felemban, F.K. Shaikh, U.M. Qureshi, A.A. Sheikh, S.B. Qaisar, Underwater sensor network applications: a comprehensive survey, Int. J. Distributed Sens. Netw. 11 (2015) 1−14.

[30] C.E. Shannon, Communication in the presence of noise, Proceedings of the IRE 37 (1949) 10−21.

[31] R.V. Hartley, Transmission of information 1, Bell Sys. Tech. J. 7 (1928) 535−563.